

# The structure of chromatophores from purple photosynthetic bacteria fused with lipid-impregnated collodion films determined by near-field scanning optical microscopy

Vladimir P. Shinkarev<sup>a</sup>, Robert Brunner<sup>c,1</sup>, Jeffrey O. White<sup>c</sup>, Colin A. Wraight<sup>a,b,\*</sup>

<sup>a</sup> Department of Plant Biology, University of Illinois at Urbana-Champaign, 190 ERML, 1201 W. Gregory Drive, Urbana, IL 61801, USA

<sup>b</sup> Department of Biochemistry, University of Illinois at Urbana-Champaign, 190 ERML, 1201 W. Gregory Drive, Urbana, IL 61801, USA

<sup>c</sup> Frederick Seitz Materials Research Laboratory, University of Illinois at Urbana-Champaign Urbana, IL, USA

Received 5 March 1999; received in revised form 19 April 1999

**Abstract** Lipid-impregnated collodion (nitrocellulose) films have been frequently used as a fusion substrate in the measurement and analysis of electrogenic activity in biological membranes and proteoliposomes. While the method of fusion of biological membranes or proteoliposomes with such films has found a wide application, little is known about the structures formed after the fusion. Yet, knowledge of this structure is important for the interpretation of the measured electric potential. To characterize structures formed after fusion of membrane vesicles (chromatophores) from the purple bacterium *Rhodobacter sphaeroides* with lipid-impregnated collodion films, we used near-field scanning optical microscopy. It is shown here that structures formed from chromatophores on the collodion film can be distinguished from the lipid-impregnated background by measuring the fluorescence originating either from endogenous fluorophores of the chromatophores or from fluorescent dyes trapped inside the chromatophores. The structures formed after fusion of chromatophores to the collodion film look like isolated (or sometimes aggregated, depending on the conditions) blisters, with diameters ranging from 0.3 to 10  $\mu\text{m}$  (average  $\approx 1 \mu\text{m}$ ) and heights from 0.01 to 1  $\mu\text{m}$  (average  $\approx 0.03 \mu\text{m}$ ). These large sizes indicate that the blisters are formed by the fusion of many chromatophores. Results with dyes trapped inside chromatophores reveal that chromatophores fused with lipid-impregnated films retain a distinct internal water phase.

© 1999 Federation of European Biochemical Societies.

**Key words:** Near-field scanning optical microscopy; Chromatophore; Membrane fusion; Sulforhodamine B; Rhodamine 6G; *Rhodobacter sphaeroides*

## 1. Introduction

Phospholipid layers supported on thin artificial films have been frequently used for electrometric measurements of the electrogenic activities of membrane proteins involved in biological energy conversions (reviewed in [1,2]). Collodion (nitrocellulose) films, which have a large capacitance and adequate mechanical stability, have been found to be especially useful when a fast time resolution of electrogenic activity is

needed [1]. In particular, such films have been used in studies of bacteriorhodopsin [3,4], photosynthetic reaction centers from purple bacteria [5–7], photosystem I [8,9], photosystem II [10], cytochrome *bc*<sub>1</sub> complexes [7,11], cytochrome oxidase [12] and others. In spite of the broad application of collodion films to electrometric measurements over the last 20 years, little is known about the structures formed after fusion of biological membranes with lipid-impregnated collodion. Using a two phase system, consisting of phospholipids in decane and water, as a model for lipid-impregnated films, Drachev et al. [13] observed the structure of chromatophores adsorbed between two phases.

To properly interpret the observed electrical properties, one should know the topology of the fused structures to the artificial film. On the basis of sensitivity of the electrical potential to gramicidin, Voitsitskii et al. [14] proposed that the structures resulting from incubation of collodion films with proteoliposomes in the presence of  $\text{Ca}^{2+}$  were blister-like with an internal water phase. However, this supposition has not been evaluated by any direct structural approaches.

Here, we used near-field scanning optical microscopy (NSOM) to study the nature of the structures resulting from fusion of chromatophores from the photosynthetic bacterium *Rhodobacter sphaeroides* to lipid-impregnated collodion film. This is the first paper where a direct structural approach is used to visualize structures formed during fusion of chromatophores with collodion films.

## 2. Materials and methods

### 2.1. Isolation of chromatophores

*R. sphaeroides* Ga cells were disrupted by a single pass through a French press in the presence of a small amount of DNase. Chromatophores were isolated in 10 mM HEPES (pH 7.5) by a differential centrifugation as described elsewhere [7].

### 2.2. Dyes

Sulforhodamine B was obtained from Molecular Probes (Eugene, OR, USA). Rhodamine 6G was obtained from Exciton (Dayton, OH, USA).

### 2.3. Labelling procedures

To trap dye inside of chromatophores, cells were pre-incubated with 20  $\mu\text{M}$  dye (rhodamine 6G or sulforhodamine B) for at least 1 h at room temperature prior to French pressing.

### 2.4. Preparation of collodion-supported membranes for image analysis

The collodion film was formed on the surface of water from a drop (10  $\mu\text{l}$ ) of 1% solution of collodion in isoamyl acetate. After formation ( $\approx 1 \text{ min}$ ), the film was picked up either on a glass slide or on a small piece of nitrocellulose filter with a small hole (5 mm). In the latter

\*Corresponding author. Fax: (1) (217) 244 1336.  
E-mail: cwraight@uiuc.edu

<sup>1</sup> Present address: Carl-Zeiss-Jena GmbH, Tatzendpromenade 1a, 07740 Jena, Germany.

**Abbreviations:** HEPES, 4-(2-hydroxyethyl)-1-piperazine-ethanesulfonic acid; NSOM, near-field scanning optical microscopy

case, the collodion film clung to both sides of the filter covering the hole with a double thickness.

We were unable to image the same collodion films used for electrometric measurements [1,2], because they disintegrated upon disassembling the electrometry cell. Instead, we used two different approaches.

**2.4.1. Vertical fusion in the solution.** The first setup (Fig. 1A) was designed to duplicate the conditions of vertical fusion inside the teflon cell used for electrometric measurements. We reproduced the fusion technique and conditions in a small beaker where the lipid-impregnated (10  $\mu$ l of 100 mg/ml azolectin in decane) collodion film was held vertically in a bulk solution containing chromatophores. After fusion of chromatophores to the collodion film in the presence of 20 mM  $\text{Ca}^{2+}$  for about 30 min, the Millipore filter with collodion film was transferred onto the glass slide and air-dried before imaging.

The disadvantage of this method includes the small fraction of membranes left intact after stirring and further transferring them onto the glass slide.

**2.4.2. Horizontal fusion to collodion film on a glass surface.** The instability of the collodion film evident in the first method was circumvented by the following modification (see Fig. 1B). After the collodion film was formed on the water surface, it was transferred to a glass slide, where it was dried for at least 1 h. The dry collodion film was impregnated, from the top only, with 10  $\mu$ l of lipid (100 mg/ml azolectin in decane) and 100  $\mu$ l of the chromatophore solution was added on top of the lipid. Fusion was induced by adding 20 mM  $\text{CaCl}_2$  to the drop and mixing the sample carefully using a pipette. Alternatively,  $\text{Ca}^{2+}$  was added to the chromatophore suspension just prior to placing it on the lipid-impregnated collodion film. After 10–20 min, 400  $\mu$ l of the 10 mM HEPES, pH 7.5 (without  $\text{Ca}^{2+}$ ) was placed on the slide nearby and mixed slowly with the first drop. The liquid was then removed by tipping the glass.

By measuring the same sample at different times after removal of aqueous medium, we found that fused structures do not change their shape or size significantly during the first 2–3 h, when kept in a closed box. In the majority of cases, using horizontal fusion, we measured the topography of structures formed on the collodion film within 1–2 h after removal from aqueous medium, to minimize any changes that might occur during drying of the sample.

## 2.5. NSOM

NSOM combines a high optical resolution with the possibility of measuring the sample topography [15]. To achieve this spatial resolution, a very small aluminum-coated glass fiber tip with a hole smaller than the wavelength of light is scanned near ( $< 20$  nm) the surface of interest. The light from the tip is collected by a microscope objective and its intensity is measured by a photodetector. The size of the hole (typically about 100 nm) determines the lateral optical resolution of the method.

A constant distance between the tip and sample is maintained by a shear force feedback technique [16,17]. In this method, the fiber tip is vibrated laterally with a frequency typically between 20 and 100 kHz and the vibration damping, arising from the long range interaction of the tip and sample interface, is measured by a piezoelectric detection system to determine the vertical position of the tip [18]. This non-contact interaction allows measurement of the topography of surfaces

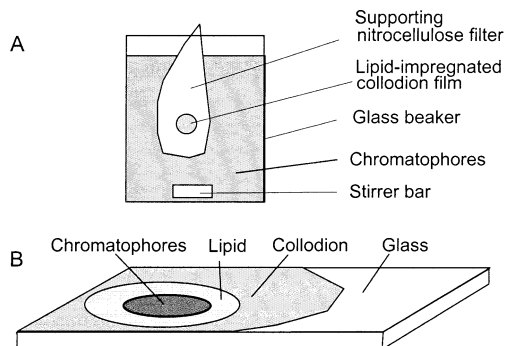


Fig. 1. Two methods used for the  $\text{Ca}^{2+}$ -induced fusion of chromatophores with collodion film. A, vertical fusion of chromatophores to collodion film. B, horizontal fusion of chromatophores with collodion film on a glass surface.

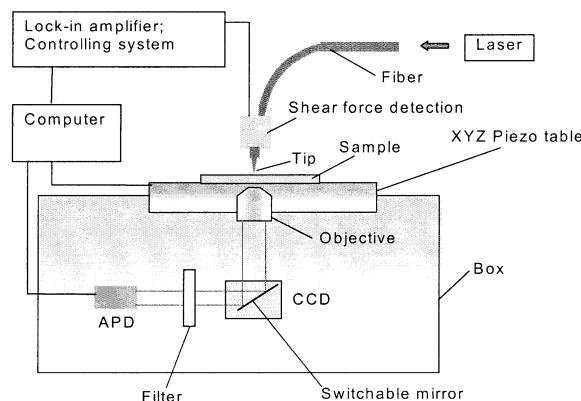


Fig. 2. Block diagram of NSOM. The light from the tip goes through the objective to the switchable mirror and then to either a CCD camera or an APD. APD, avalanche photodiode; CCD, charge-coupled device.

of soft samples without damage with a horizontal resolution  $< 30$  nm and a vertical resolution  $< 1$  nm [18]. It also allows measuring under water.

In this work, we used a commercial near-field optical microscope from Witec (Ulm, Germany). The block diagram of the near-field scanning optical microscope used in this work is shown in Fig. 2. The fluorescence was excited at 488 or 514 nm by an argon-ion laser (ILT, USA) and at 400 nm by a frequency-doubled Ti-sapphire laser (Spectra-Physics, USA). Fluorescence detection was provided by an avalanche photodiode (single photon counting module SPCM-100-PQ, EG and G, USA). Optical filters between the objective and detector separated fluorescence from excitation.

Images were acquired using the software Winscan 2.01 (I. Hörsch, Taunusstein, Germany) and were processed by both Winscan 2.01 and by SXMImage (O. Marti, Ulm, Germany) software.

## 3. Results

### 3.1. NSOM images of collodion film

We first examined the NSOM images of pure collodion film on a glass slide, in the absence of lipid impregnation (Fig. 3A, B). The topography image (Fig. 3A) shows that the collodion is a solid film, sometimes with stripes (originating from folding of the collodion film during transfer onto the glass slide surface), volcano-like defects (possibly originating during isoamylacetate evaporation from the hardening surface of nitrocellulose) and smaller ( $\leq 0.5$   $\mu$ m) granular structures with heights of about 0.01  $\mu$ m. The fluorescence of the collodion film was weak and only stripes and bigger volcano-like defects can be seen (Fig. 3B).

### 3.2. NSOM images of lipid-impregnated collodion film

Impregnation of the collodion by azolectin in decane and subsequent exposure to  $\text{CaCl}_2$  solution led to the appearance of a network of small ( $\leq 0.5$   $\mu$ m) rounded structures with heights of about 0.01  $\mu$ m, which almost completely cover the surface (Fig. 3C). The fluorescence was weak and there was no clear correspondence between the topography and fluorescence. This appearance of structures (Fig. 3C), even in the absence of the chromatophores, complicates identification of structures arising from fusion of chromatophores with lipid-impregnated collodion film.

### 3.3. NSOM images of chromatophores on the collodion film

The coverage of the lipid-impregnated collodion film by

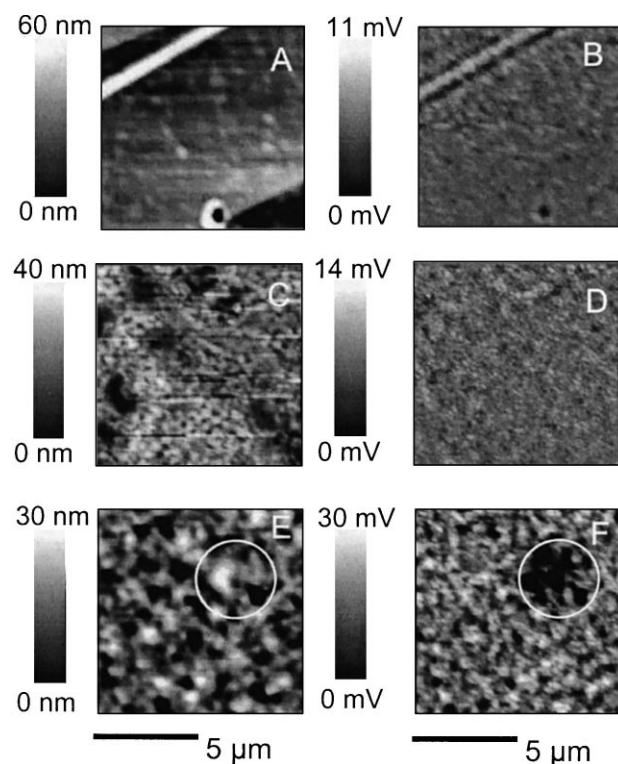


Fig. 3. NSOM images of dry collodion film on a glass slide (A and B), of wet lipid-impregnated collodion film in the presence of  $\text{Ca}^{2+}$  (C and D) and of chromatophores horizontally fused with lipid-impregnated collodion film (E and F). A, C and E show the surface topography of the samples. B, D and F show the fluorescence (excitation at 400 nm, measurement with orange filter OC12,  $\lambda > 540$  nm). Circles in E and F indicate the photobleached region.

chromatophores depends on many factors, such as the concentration of chromatophores, the time of fusion,  $\text{Ca}^{2+}$  concentration, etc. In different samples, we observed both low and high coverage of the collodion film by chromatophores.

Fig. 3E, F show NSOM images of chromatophores from *R. sphaeroides* horizontally fused to a lipid-impregnated collodion film. Both the topography and fluorescence indicate the presence of a heterogeneous population of granular structures with sizes ranging from 0.2 to 1 micron. The topography mode of NSOM shows their heights to be 10–40 nm. The fluorescence emission intensity is significantly higher after fusion with chromatophores and there is a general consistency between the topography and fluorescence images, consonant with emission from the various pigments of photosynthetic membranes.

The fluorescence from the chromatophore-fused samples undergoes photobleaching by the light ( $\lambda = 400$  nm) passing through the aperture of the probe, if the sample is exposed for more than 5–10 min (see field marked by circle in Fig. 3F). We were unable to photobleach the weakly fluorescent lipid-impregnated collodion film without chromatophores, even with much longer exposure times. This is consistent with a much smaller light absorption by the lipid compared to the pigment-rich chromatophores. Thus, we conclude that the structures seen in Fig. 3E, F are due to chromatophores attached to the lipid-impregnated collodion film.

To avoid photobleaching of chromatophores, the fluorescence was excited at 488 or 514 nm by an argon-ion laser. However, we found that in this case, intrinsic fluorescence

from small structures is below our detection and only large structures, which were rarely encountered ( $< 1\%$ ), showed a detectable fluorescence. To see smaller structures in the fluorescence mode, we used fluorescent dyes.

#### 3.4. Fusion of chromatophores with rhodamine 6G trapped inside

Addition of rhodamine 6G to isolated chromatophores before fusion did not lead to an enhanced fluorescence from the blisters. Instead, the dye appeared to accumulate at the margins of the larger structures, apparently concentrating there as the sample dried (not shown).

To incorporate dye inside the chromatophores, we incubated the bacterial cell suspension with dye for  $> 1$  h, before chromatophore isolation.

Fig. 4A, B show the NSOM images of a typical chromatophore preparation with rhodamine 6G trapped inside. Good correspondence between the topography and fluorescence images is seen. The fluorescence from smaller structures is quite variable, possibly because of the small and variable number of dye molecules trapped.

Fig. 4A, B show a significant heterogeneity in the size distribution of the structures formed by fusion of chromatophores with lipid-impregnated collodion film. The largest blis-

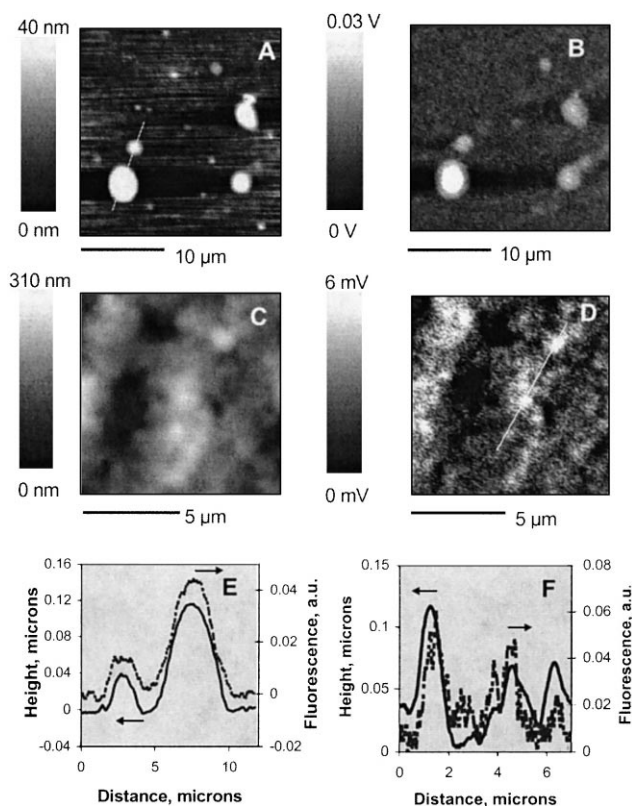


Fig. 4. NSOM images of *R. sphaeroides* chromatophores isolated from cells incubated with rhodamine 6G (A and B) or sulforhodamine B (C and D), fused with lipid-impregnated collodion film. A and C, surface topography of the samples. B, fluorescence of the sample (shown in A), excited at 488 nm and measured using an OC12 filter. D, fluorescence of the sample (shown in C) excited at 514 nm and measured using an OC13 filter. E, cross-section of two bubbles (shown by a white bar in A) for topography (solid line) and fluorescence (dashed line). F, cross-section of the images (shown by a white bar in D) for topography (solid line) and fluorescence (dashed line).

ter seen here is about 4 microns in diameter while the smallest is about 0.5 micron. We suspect that large blisters are the result of fusogenic activity of the positively charged rhodamine 6G, leading to the fusion of chromatophores in solution, even before the addition of  $\text{Ca}^{2+}$ .

Trapping of rhodamine 6G inside the chromatophores indicates that the structures formed after fusion of chromatophores with lipid-impregnated collodion film are indeed blisters, with a definite aqueous interior. However, the absence of detectable fluorescence from small ( $< 1 \mu\text{m}$ ) structures and the presence of fluorescence outside chromatophores suggest that rhodamine 6G can penetrate the hydrophobic membrane and cannot be completely trapped in chromatophores. It is possible that the positively charged dye rhodamine 6G is actively excluded (pumped out) from the interior of the chromatophores by the membrane potential generated by the light-induced activity of the photosynthetic apparatus, still active in the wet sample.

### 3.5. Fusion of chromatophores with sulforhodamine B trapped inside

To further test for the presence of a water phase inside the fusion structures, we used the negatively charged dye sulforhodamine B, which cannot readily penetrate the membranes.

Fig. 4C, D show the NSOM images of fused chromatophores isolated from cells incubated with sulforhodamine B. There is a strong positive correlation between topography and fluorescence images, which contrasts sharply with the control experiment in which sulforhodamine B was added to the chromatophores from the outside (not shown).

Trapping of negatively charged sulforhodamine B inside the chromatophores provides strong evidence that the structures formed after fusion of chromatophores with lipid-impregnated collodion film are indeed blisters with an internal water phase.

### 3.6. NSOM images of chromatophores vertically fused with a lipid-impregnated collodion membrane

In the case of horizontal fusion of chromatophores to collodion film (Figs. 3 and 4), it is difficult to exclude a constituting role for the sedimentation of chromatophores and their aggregates on the collodion surface. To provide control for the artifacts arising from horizontal fusion, we imaged vertically fused chromatophore films, where the possibility of sedimentation of chromatophore aggregates on the collodion surface is minimal. Vertical fusion also more closely corresponds to the standard geometry in the electrometry cell (Skulachev, 1988).

Fig. 5 shows a representative NSOM image of such chromatophores. The size of the fusion structures ranges from about 0.3 to 2 microns (average about  $1 \mu\text{m}$ ), while their height ranges from 0.02 to 0.06 microns (average about  $0.03 \mu\text{m}$ ). In general, the images of chromatophores vertically fused with a collodion membrane are similar to those for the horizontal fusion.

However, we note the following three differences. (a) The height of the final structures in the case of vertical fusion was more homogeneous and never exceeded 100 nm, while for horizontal fusion, structures as high as 1 micron were observed, possibly due to sedimentation of chromatophores and their aggregates. (b) The structures formed by vertical fusion have a wider base, possibly due to membrane flow under the influence of gravity forces. (c) In the case of vertical

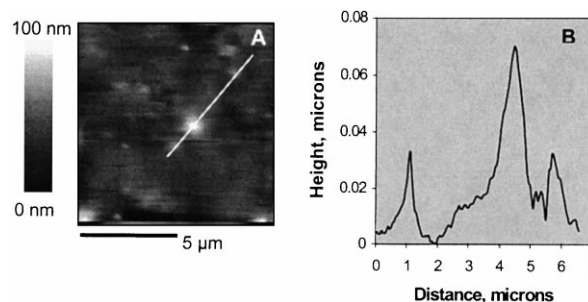


Fig. 5. NSOM image of *R. sphaeroides* chromatophores vertically fused with lipid-impregnated collodion membrane. A, topography of the sample. B, cross-section of the topography image (shown by a white bar in A).

fusion, we did not observe any 'bubble on bubble' structures, while this kind of structure is frequently seen in horizontal fusions (see, e.g. Fig. 4C).

## 4. Discussion

The NSOM images reveal a wide range of sizes of the structures resulting from fusion of chromatophores with collodion lipid film. Because the image area cannot exceed  $100 \mu\text{m} \times 100 \mu\text{m}$  and the time required for the scan (approximately 1 h), the statistical sampling is limited. Nevertheless, in all samples, single blisters had diameters ranging from 0.3 to  $15 \mu\text{m}$  (average  $\approx 1 \mu\text{m}$ ) and heights from 0.01 to  $1.2 \mu\text{m}$  (average  $\approx 0.03 \mu\text{m}$ ), indicating that many chromatophores can be fused together to form a blister.

If we assume that a chromatophore has a diameter of about  $100 \text{ nm}$  [19], the surface of the chromatophore will be  $4\pi R^2 \approx 1.2 \times 10^5 \text{ nm}^2$ . The average single blister observed by NSOM for vertical fusion had a radius,  $R_1$ , of about  $1 \mu\text{m}$  and a height,  $h$ , of about  $0.03 \mu\text{m}$ . The surface of such a blister is approximately  $\pi(R_1^2 + h^2) \approx 3 \times 10^6 \text{ nm}^2$ . Thus, we estimate that as many as 20–25 chromatophores would need to be fused to create an average blister. These values may be over-estimates, however, as transfer of lipid from the collodion film to the fusion sites would reduce the number of chromatophores required to produce the sizes observed.

Another question with important consequences for the electrometric measurements is the fraction of the surface covered by blisters. In some films, we observed almost complete coverage of the membrane by chromatophores (see Fig. 3E). However, in many others, the fraction of membrane covered by detectable fusion structures was less than 0.05. This small fraction of surface covered by blisters indicates that the measured electric potential can be 20 times less than the maximum. We intend to use NSOM to find optimal conditions for the fusion of membrane vesicles with lipid-impregnated films and to correlate this with the amplitude of the photoelectric response of chromatophores in the electrometric assay.

**Acknowledgements:** This work was supported by NIH Grant GM53508 and by Department of Energy Grant DEFG02-ER9645439.

## References

- [1] Skulachev, V.P. (1982) *Methods Enzymol.* 88, 35–45.
- [2] Skulachev, V.P. (1988) *Membrane Bioenergetics*. Springer-Verlag, Berlin.

- [3] Drachev, L.A., Kaulen, A.D., Khitrina, L.V. and Skulachev, V.P. (1981) *Eur. J. Biochem.* 117, 461–470.
- [4] Kaulen, A.D., Drachev, L.A. and Zorina, V.V. (1990) *Biochim. Biophys. Acta* 1018, 103–113.
- [5] Drachev, L.A., Semenov, A.Y., Skulachev, V.P., Smirnova, I.A., Chamorovsky, S.K., Kononenko, A.A., Rubin, A.B. and Uspenskaya, N.Y. (1981) *Eur. J. Biochem.* 117, 483–490.
- [6] Chamorovsky, S.K., Drachev, A.L., Drachev, L.A., Karagul'yan, A.K., Kononenko, A.A., Rubin, A.B., Semenov, A.Y. and Skulachev, V.P. (1985) *Biochim. Biophys. Acta* 808, 201–208.
- [7] Drachev, L.A., Kaurov, B.S., Mamedov, M.D., Mulkidjanian, A.J., Semenov, A.Y., Shinkarev, V.P., Skulachev, V.P. and Verkhovsky, M.I. (1989) *Biochim. Biophys. Acta* 973, 189–197.
- [8] Mamedov, M.D., Gadzhieva, R.M., Gourovskaya, K.N., Drachev, L.A. and Semenov, A.Y. (1996) *J. Bioenerg. Biomembr.* 28, 517–522.
- [9] Vassiliev, I.R., Jung, Y.S., Mamedov, M.D., Semenov, A.Y. and Golbeck, J.H. (1997) *Biophys. J.* 72, 301–315.
- [10] Mamedov, M.D., Lovyagina, E.R., Verkhovsky, M.I., Semenov, A.Y., Cherepanov, D.A. and Shinkarev, V.P. (1994) *Biochemistry (Russia)* 59, 685–689.
- [11] Semenov, A.Y., Bloch, D.A., Crofts, A.R., Drachev, L.A., Genis, R.B., Mulkidjanian, A.Y. and Yun, C.H. (1992) *Biochim. Biophys. Acta* 1101, 166–167.
- [12] Zaslavsky, D.L., Smirnova, I.A., Siletsky, S.A., Kaulen, A.D., Millet, F. and Konstantinov, A.A. (1995) *FEBS Lett.* 359, 27–30.
- [13] Drachev, L.A., Kaulen, A.D., Samuilov, V.D., Severina, I.I., Semenov, A.Y., Skulachev, V.P. and Chekulaeva, L.N. (1979) *Biophysics* 24, 1063–1071.
- [14] Voitsitskii, V.M., Drachev, L.A., Kaulen, A.D. and Skulachev, V.P. (1979) *Bioorg. Chem. (Russia)* 5, 1184–1195.
- [15] Paesler, M.A. and Moyer, P.J. (1996) *Near-field Optics Theory, Instrumentation and Applications*. Wiley, New York.
- [16] Toledo-Crow, R., Yang, P.C., Chen, Y. and Vaez-Iravani, M. (1992) *Appl. Phys. Lett.* 60, 2957–2959.
- [17] Betzig, E., Finn, P.L. and Weiner, J.S. (1992) *Appl. Phys. Lett.* 60, 2484–2486.
- [18] Brunner, R., Bietsch, A., Hollricher, O. and Marti, O. (1997) *Rev. Sci. Instrum.* 68, 1769–1772.
- [19] Wang, Z.Y., Kudoh, M., Ohama, Y., Nakatani, H., Kobayashi, M. and Nozawa, T. (1997) *Photosynth. Res.* 51, 51–59.